# PARTICLE CHARACTERISATION OF RAIL SANDS FOR UNDERSTANDING TRIBOLOGICAL BEHAVIOUR

W.A. Skipper[1], S. Nadimi[2,3], A. Chalisey[4], R. Lewis[1]

[1] Centre for Doctoral Training in Integrated Tribology, The University of Sheffield, Sheffield, UK
[2] School of Engineering, Newcastle University, Newcastle upon Tyne, UK
[3] Faculty of Engineering, University of Leeds, Leeds, UK
[4] RSSB, The Helicon, One South Place, London, UK

**ABSTRACT**: Low adhesion between a train's wheel and the rail can cause performance and safety issues, costing the UK rail industry ~£345 m/annum. Sand is applied to the wheel/rail interface to increase traction when low adhesion conditions are present. In order to improve performance, an understanding of how particles are entrained into and act within the interface is needed. This paper outlines a particle characterisation framework and applies it to sands used in the rail industry: Leighton Buzzard (LB), Central European (CE), and Derbyshire Youlgreave (DY) sand. The largest difference found in this framework was between the sand's particle size, LB being largest, then CE, then DY. A high pressure torsion rig measured traction when the sands were applied to dry, wet, and leaf extract contaminated conditions, the latter two representing low adhesion conditions. All sands had no impact on wheel/rail adhesion in dry conditions; in low adhesion conditions DY had little influence, whereas LB and CE were found to increase traction. Particles in dry conditions had no effect on test specimen surface roughness, whereas roughness increased when sand was applied in low adhesion conditions. The developed characterisation framework provides a platform for assessing prospective adhesion enhancing particles.

**KEYWORDS**: Traction enhancement; Braking; Sanding; Particle characterisation; Tribological testing.

# 1 INTRODUCTION

Low adhesion[1] between train wheels and the rail is estimated to cost the UK industry £345m per annum [1] with the majority of this cost coming during Autumn when weather conditions are sub-optimal. Low adhesion in the wheel/rail contact leads to costly delays [2] as well as safety issues due to the loss of traction when braking, potentially leading to SPADs (signals passed at danger) and in the worst case collisions [3]. Low adhesion becomes a major problem when the coefficient of traction between wheel and rail drops below 0.2 for acceleration and 0.09 for braking [2]. Low adhesion conditions can exist in the wheel/rail contact when lubrication is created by a present third body layer, such as: water [4], water and iron oxides [5], and leaves on the line which bond tightly to the rail, thereby making it hard to restore the surface to its clean condition [6].

As the cost of low adhesion is so high it is imperative that mitigation is applied to the wheel/rail interface to enhance traction/braking. One of the methods for achieving this is sanding which has been in use for many years. Sanding is a train-borne system that activates whenever low adhesion is detected; the sand particles are discharged into the wheel/rail contact from a hopper via a hose directed at the contact in the opposite direction of travel. A schematic of a typical sander is shown in **Error! Reference source not found.**.

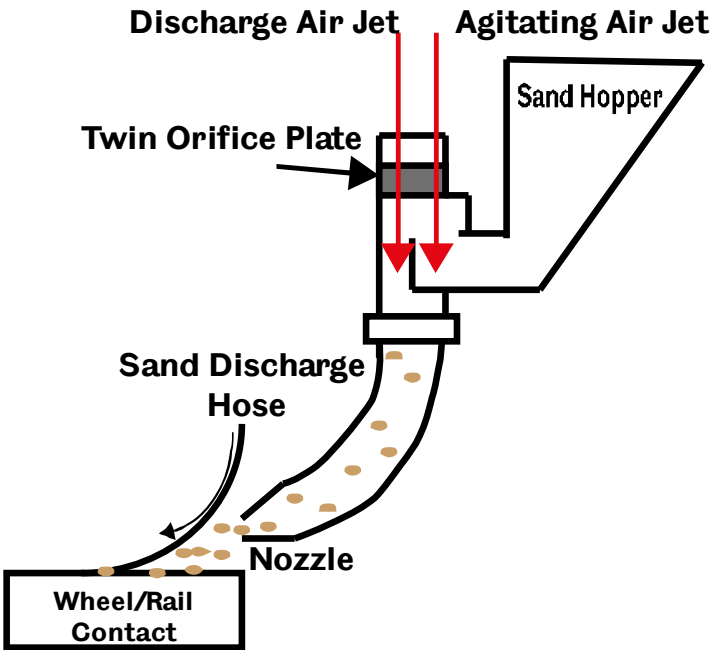


*Figure 1- Schematic of Typical Sander.*

In a literature review [7] looking at the effect of sand characteristics on traction restoration it was found that previous research primarily focussed on the grain size of the sand [8]–[12]. Some research has also been conducted looking at the effect of particle hardness on restoring traction [13]. These studies suggested that larger particle sizes were more effective at restoring traction/braking, but there did seem to be an upper limit at which larger particles were not being effectively entrained into the contact. There was also some evidence to suggest harder particles were more effective, but this relationship plateaued after the hardness went above that of quartz.

[1] In the railway industry “adhesion” or “adhesion coefficient” is defined as the amount of traction present when the wheel/rail contact enters partial slip. In this paper the terms can be considered synonymous.

This paper aims to define a characterisation framework for measuring the relevant properties of sand particles and assessing their effect on mitigation of adhesion loss, using a small scale tribological test. This framework will allow future particle systems to be identified for possible use in sanding applications.

Previous studies have largely ignored the particle geometry, mineralogy, and physical properties, all of which may have an effect on the traction recovery in the wheel/rail contact and on the particle entrainment into the contact. The characterisation framework in this paper utilises a series of tests to assess these properties.

In addition, a small scale test is used to assess the coefficient of traction of the rail sands in dry, wet, and sycamore leaf extract contaminated conditions to assess their traction restoring capability and how the particle properties relate to this effect.

## 2 PARTICLE CHARACTERISATION

Three different types of sand are characterised here, to better understand how particle characteristics affect the level of traction in the wheel/rail contact. The sands characterised were:

- Leighton Buzzard (LB); the current industry standard for sand used by the UK rail industry. Garside sand meets all the current sanding standards as set out in GMRT2461 [14].
- Central European (CE); currently used by train operators on the central European rail system.
- Derbyshire Youlgreave (DY); currently sold as an “anti-skid” sand by Derbyshire Aggregates Ltd.

Images of these sands are shown in Figure 2. Representative samples of these sands were obtained using a chute splitter (as outlined in ASTM C702 [15]) which reduces particle size variations between sand particle samples to <5% [16].

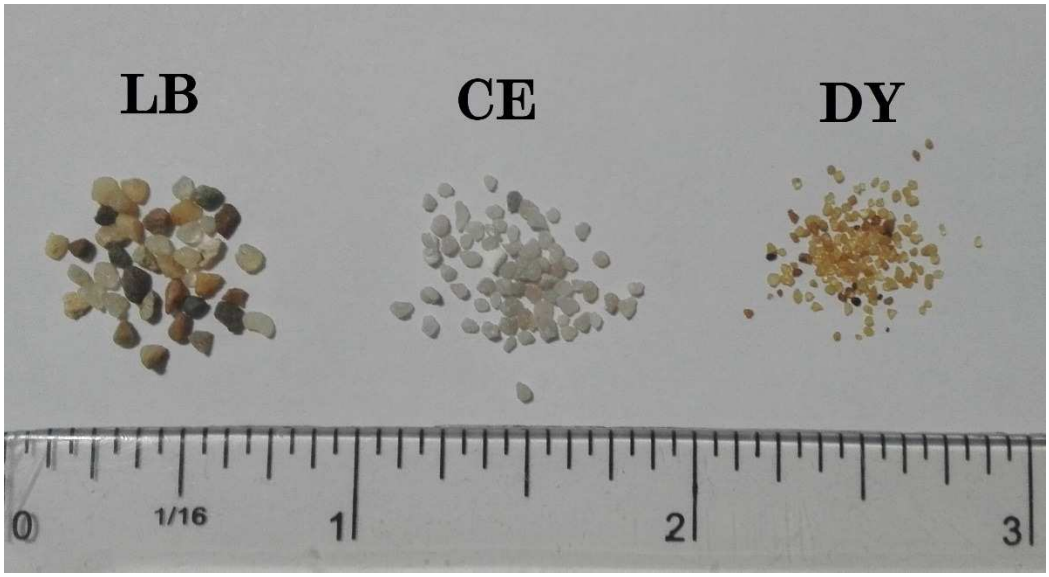


*Figure 2- Photos of Tested Sands (Scale at Bottom in centimetres).*

## 2.1 Particle Size and Shape

To characterise the particle size and shape, sieve and image analyses have been carried out. The sieve analysis shows the particle size distribution ranging from 0.3 to 2 mm (Figure 3). It can be seen that DY sand is slightly out of the range proposed by the UK guideline for rail sand [14]. Table 1 gives the particle size distribution characteristics, obtained by sieving, showing around 400 µm difference in D50.

It has been well established that particle shape has a significant impact on dynamic and quasi-static behaviour of particles [17]–[19]. Here, a representative sample of each type of sand was characterised by a Morphologi G3 (Malvern Panalytical Ltd., Malvern, UK). The particles were dispersed on a slide at 4 Barg with 10 ms of pressure pulse injection time. This was kept constant for all samples.

The image analysis was carried out to characterise circularity, convexity and circle equivalent diameter. As can be seen in Figure 4, all sands show circularity distribution from 0.4 to 1. Elongation distribution is shown in Figure 5; particles show a similar amount of elongation, between 0-0.5. Convexity distribution is shown in Figure 6; particles show almost similar convexity. A gap in both the circularity and the convexity distribution of LB sand can be seen from 0.7 to 0.8 and from 0.9 to 0.95 respectively. Circle Equivalent diameter is presented in Figure 7, showing a similar trend to sieve analysis with a wider gap between each distribution.

*Table 1- Characteristic Measures of the Particle Size Distribution of the Three Sands, obtained by Sieve Analysis.*

| | **CE** | **DY** | **LB** |
|---|---|---|---|
| **D10 (µm)** | 722 | 376 | 811 |
| **D50 (µm)** | 952 | 557 | 1437 |
| **D90 (µm)** | 1170 | 1032 | 1888 |

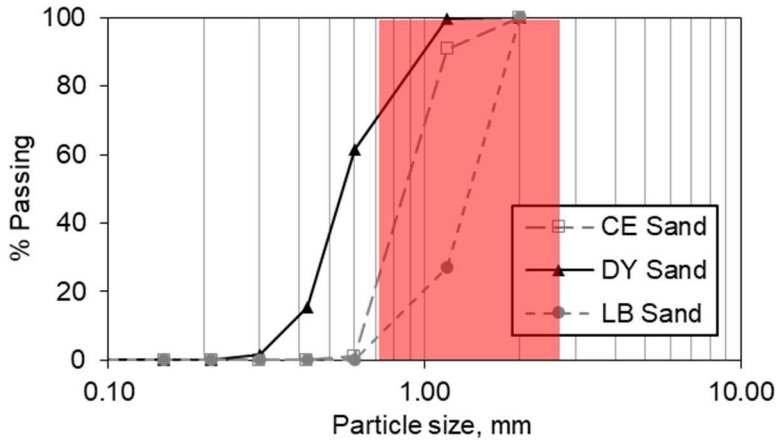


*Figure 3- Particle Size Distribution of Three Sand Types used in this Study obtained by Sieve Analysis. The Red Area shows the Size Range currently accepted by UK standards [14].*

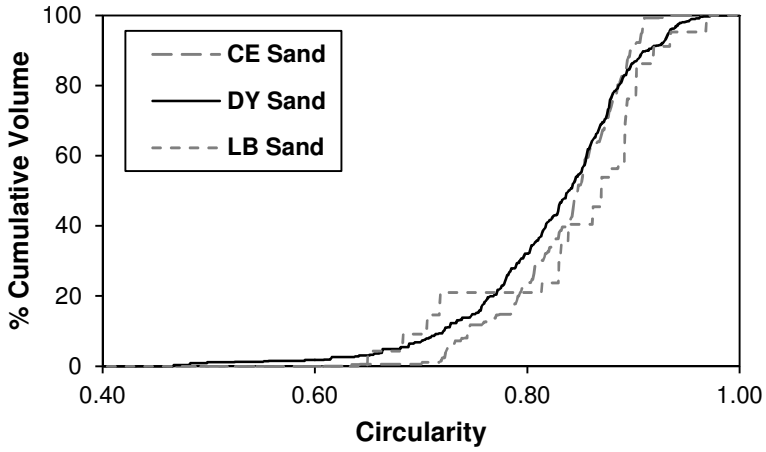


*Figure 4- Circularity Cumulative Volumes of Three Sand Types used in this Study obtained from Morphologi G3.*

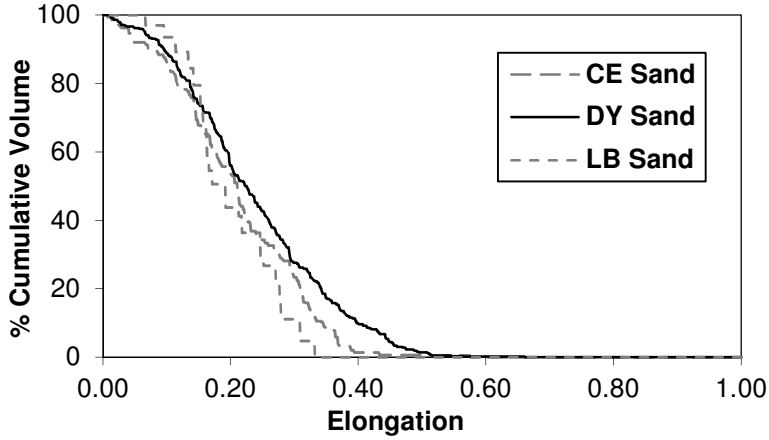


*Figure 5- Elongation Cumulative Volumes of Three Sand Types used in this Study obtained from Morphologi G3.*

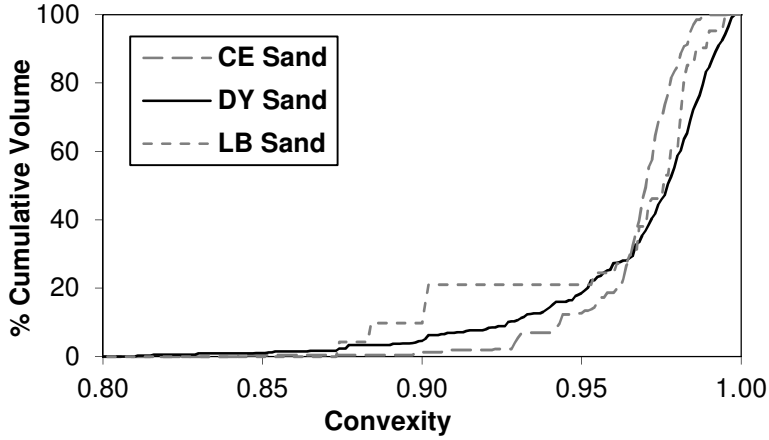


*Figure 6- Convexity Cumulative Volumes of Three Sand Types used in this Study obtained from Morphologi G3.*

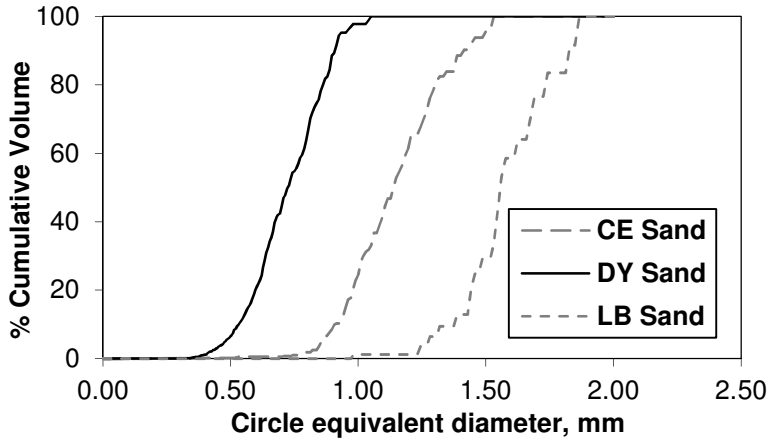


*Figure 7- Circle Equivalent Cumulative Volumes of Three Sand Types used in this Study obtained from Morphologi G3.*

## 2.2 Mineralogy

X-ray diffraction (XRD) measurements of each type of sand were used to ascertain the major constituent minerals. The measurements were carried out using a Siemens D5000 X-ray diffractometer and were scanned using Cu $K\alpha_1$ radiation between slit angles of 5-80°. The data were ~~was~~ then assessed using ICDD PDF-4+ 2018 software to identify and match characteristic peaks to elements in the software database.

Both CE and DY sands were found to be made up of 100% silica, whereas LB sand was mostly silica but contained small amounts of titania. The characteristic peaks from the XRD data have been included in Figure 8.

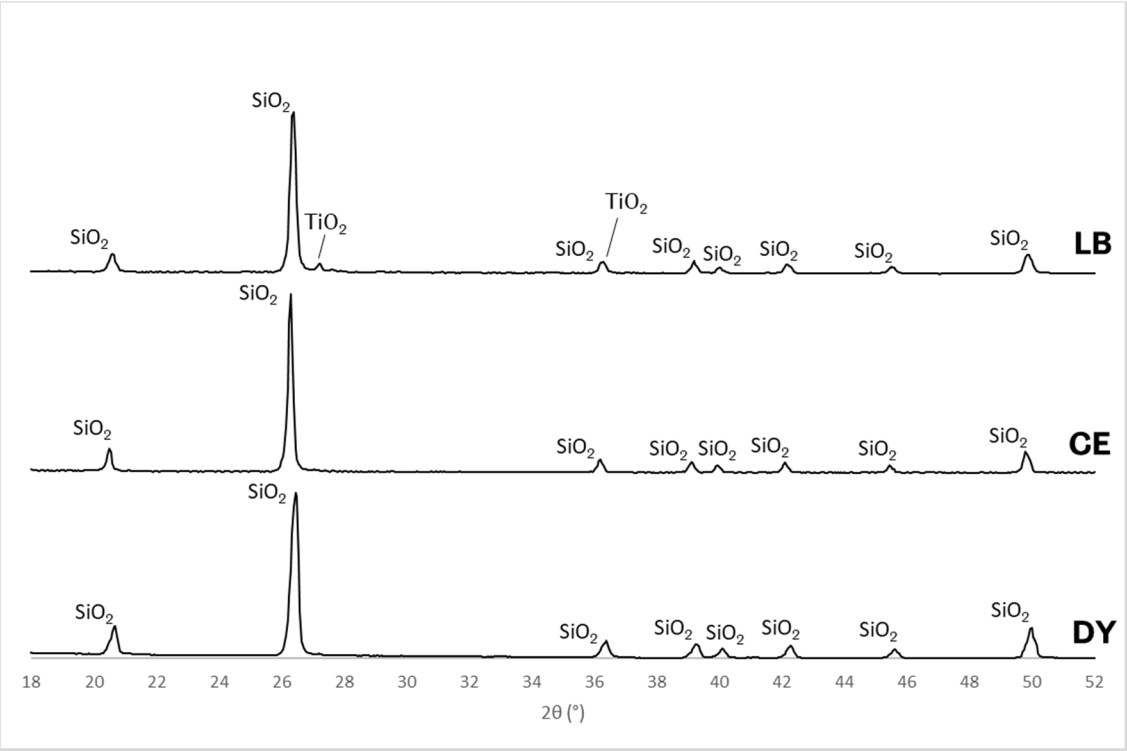


*Figure 8- XRD Data for all tested sands.*

## 2.3 Hardness and Fracture Toughness

The nano-hardness of the sand particles ~~was~~ measured by nano-indentation using the Oliver-Pharr method [20]. The particles were suspended in epoxy resin and ground and polished till a suitable surface for indentation was obtained. The indentations were carried out using the Hysitron TI Premier with a diamond Berkovich tip. A load of 10,000 μN was applied to the particles surface with four indents for each particle. The micro-hardness and fracture toughness of the particles were measured using a Struers Durascan machine with the particles being prepared in the same way as described for nanoindentation. The fracture toughness of the particles was obtained by measuring the crack length (using in-built image measuring tools in the Durascan software) caused by the indent and using these to calculate a value for fracture toughness using the method outlined by [21]; as sand is a brittle material, it can be assumed that a correlation exists between fracture toughness and a particle side-crushing stress. The hardness and fracture toughness values were similar for all particle types, both nano and micro hardness measurements gave similar hardness measurements of approximately 12 GPa. A summary of all measurements is presented in Table 2.

*Table 2- Summary of Results obtained using Indentation Techniques.*

| Sand | Nano-Hardness (GPa) | Micro-Hardness (GPa) | Fracture Toughness ($MPa/m^{0.5}$) | Stiffness (GPa) |
|---|---|---|---|---|
| **LB** | 12.2 ±2.0 | 12.5 ±0.9 | 12.5 ±4.4 | 312 ±9 |
| **CE** | 11.2 ±0.8 | 12.4 ±1.2 | 13.2 ±9.2 | 170 ±6 |
| **DY** | 13.4 ±1.0 | 13.0 ±0.6 | 12.3 ±3.2 | 400 ±9 |

## 2.4 Coefficient of Restitution

The coefficient of restitution was measured using image analysis of sand particles bouncing off a piece of rail, these images were recorded with a Phantom V210 high speed camera at frame rates of 2230 fps. 20 particles of each sand type were dropped one at a time onto the rail and there velocities immediately before and after bouncing were analysed using the mtrackJ plugin in ImageJ software.

All tested sands were found to have a coefficient of restitution of ~0.5, with all sands exhibiting large standard deviations between particles; a graphical representation of these results has been included in Figure 9. Previous full-scale testing found that entrainment of sand was largely dependent on bounce height and linear velocity [22], therefore all bounces were analysed regardless of rotational velocity.

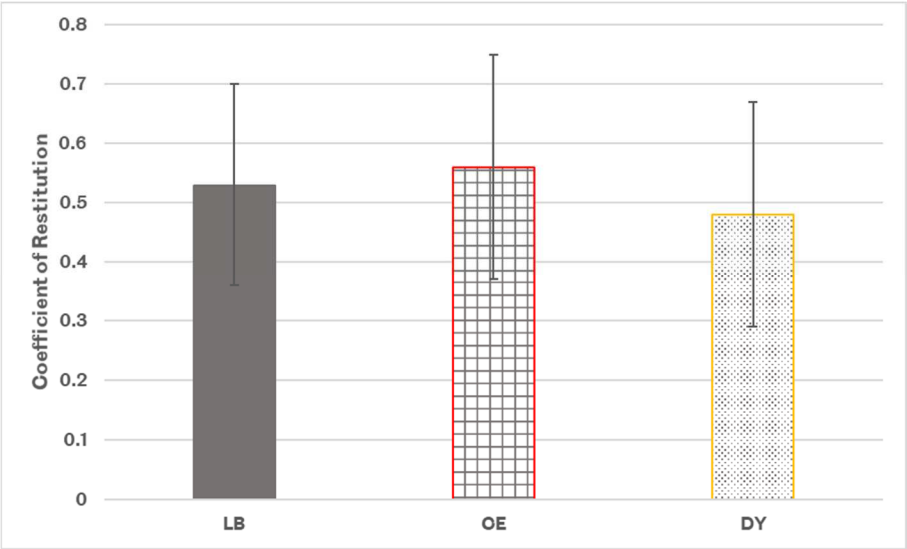


*Figure 9- Measured Coefficients of Restitution.*

## 2.5 Surface Energy

Sand particles have very low surface energy and generally are classified as cohesionless materials. However, the fine fragments produced as a result of breakage in the wheel-rail contact may adhere to the rail. Here, the interfacial adhesive surface energy of sand fragments is measured by the Drop Test Method [23], by which the particles are subjected to a transient tensile force that is produced by the impact of a steel plate, where the particles reside, being dropped onto a stopper ring whereupon larger particles come unattached; the interfacial surface energy is inferred from Johnson, Kendall and Roberts analysis [24]. A sample of test particles is dispersed on a polished steel plate of 6 mm x 6 mm and 2 mm thickness, which is stuck to an aluminium stub. The dispersion is carried out using the same procedure as for the particle shape analyses described above.

Following this step, images of particles on the steel substrate are recorded. The particles are then subjected to 1-2 m/s impact velocity, measured by a Photron FASTCAMSA5 high speed video camera at 75,000 frames per second. Three repeats are carried out for each test. In order to calculate the interfacial surface energy, the critical particle diameter, for which the force balance is made between adhesion and detachment momentum, is measured as ~85 μm for all three types of sands.

Based on the balance between the force of adhesion by JKR model and force of detachment by Newton's second law of motion, the interfacial surface energy is calculated as less than 0.1 $mJ/m^2$ for all three types of sand particles used in this study in contact with the steel plate.

# 3 BULK CHARACTERISATION

Whilst entering the wheel/rail interface the sand is dispersed out of the hose and there is little inter-particle interaction as the density of sand on the rail is relatively low (~0.15 $kg/m^2$ [25]). However, when the sand is still in the hopper the bulk characteristics of the sand become important to the sanding operation. In this section, two simple methods for assessing these bulk characteristics are described and all three sands assessed.

## 3.1 Angle of Repose

A physical measure to predict the relative flowability of particles is their angle of repose. The measurement of the angle of repose is a simple and quick method that can demonstrate

changes in the flow properties. Combining this experiment with measurements of single particle properties such as friction, adhesion, size and shape can improve our understanding of flowability characteristics. There is no general agreement on the standard method to measure the angle of repose. Descriptions of different methods is out of scope of this paper and readers can find more information elsewhere [26].

Here, the device developed by [27] is used due to availability (Figure 10(a)). A representative sample of 200+/- 0.1 gr is weighed out and gently poured on the upper chute. The vibratory motor is switched on so that the particles flow down into the metal hopper and onto the lower chute that guides the particles against the vertical wall.

Three tests have been carried out for each sample which give measurements of the angle of repose with following values: 36°+/-1° for DY sand (Figure 10(b)), 30°+/-1° for CE (Figure 10(c)) and 26°+/-1° for LB (Figure 10(d)). As mentioned above, these values are the result of combined effect of size, shape, interparticle friction, and adhesion.

(a)


(b) (c) (d)

*Figure 10- (a) Mark 4 Powder Research Ltd. AoR tester (b) DY sand, (c) CE sand, (d) LB sand.*

## 3.2 Confined Compression

Another quick way to characterise the bulk mechanical properties is bulk compression; a mechanical testing machine, here an Instron 5566 machine, with a 10kN load cell was used to compress a confined sample of sand. This test method has previously been analysed in [28]. A pre-weighted amount of sand (~60 g) was introduced into a cylindrical stainless steel die with a 40 mm diameter and then tapped to improve packing and produce the required height (25 mm). A close-fitting stainless steel piston with a small peripheral clearance in the die was used to apply the load. Die filling was carried out by air pluviation using funnel to maintain the same condition for all tests. The speed of the piston was set up at 0.1 mm/min

for all the bulk compression tests, two tests were carried out for each sand. Figure 11(a) shows the stress-strain relationship applied on the bed. As can be seen, DY sand shows lower strain in comparison with CE and LB sands which might be due to smaller particle size of DY sand. The bed of LB sands shows more rearrangement and plastic behaviour than CE sands. Four sieve cuts (850, 500, 300, and 63–) were used in the bulk compression tests. The particle size distribution after the compression is shown in Figure 11(b). Comparing with the particle size distribution for uncrushed sands (Figure 3) there appears to be little difference, suggesting the effect of particle breakage upon the applied bulk strain was negligible.

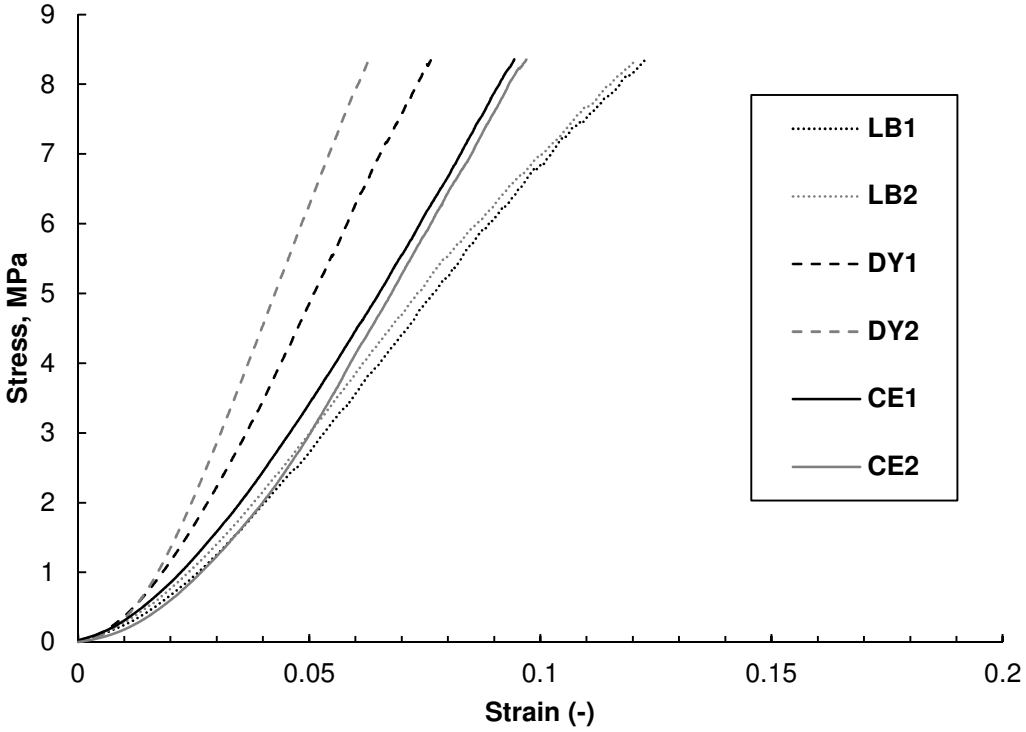


(a)

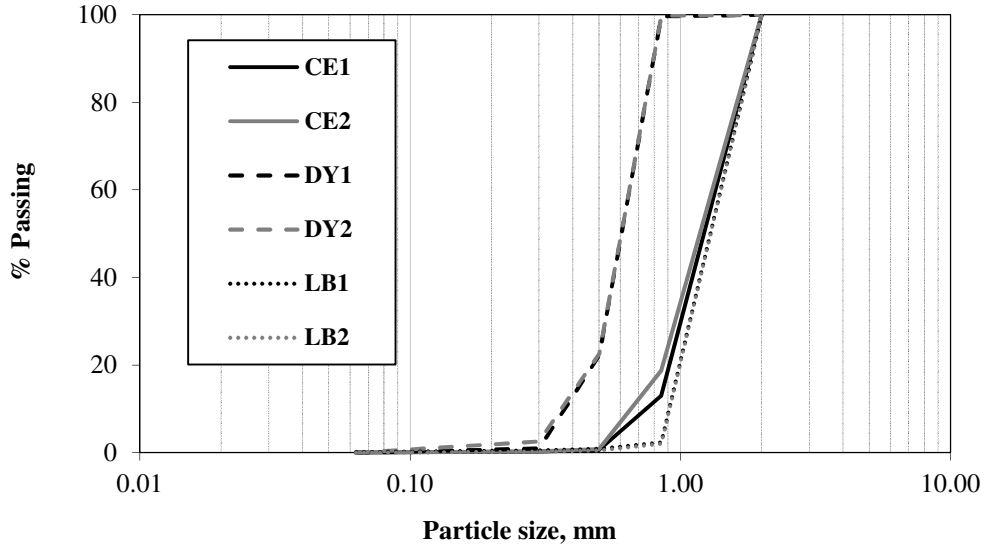


(b)

*Figure 11- (a) Stress-Displacement of confined compression experiments on three types of sands, (b) Particle Size Distribution after compression test.*

# 4 TRIBOLOGICAL TESTING

Pin-on-disc tests have been used in the past to study friction at high contact pressures (as seen in the wheel/rail contact). However, due to the small contact area used in these tests, granular materials are not appropriate as a single particle may completely dominate the contact area, leading to unrealistic results.

Twin-disc tests have also been used to study the effect of granular material on friction. However, the test is more severe than an actual scenario as more sand enters the contact than is realistic, due to the close proximity of the sand application device [29].

The high pressure torsion (HPT) rig is capable of achieving high contact pressures whilst also maintaining a large enough contact area for the particles not to dominate, and the precise control of the amount of sand being applied to the contact for each cycle allows for more realistic test conditions.

HPT rigs have been used as a bench test of the effect of different third body layers in wheel/rail contact, including iron oxides [30], top-of-rail friction modifiers [31], and sand [32]. These experimental methods were adapted for the testing conducted in this paper.

## 4.1 High Pressure Torsion

The HPT rig compresses a bottom specimen (made of R260 grade rail) together with a top specimen (made of R8T wheel) to create an annular contact. A torque is applied to the bottom specimen, under a specified normal load, N, and rotated at a low speed (<1 mm/s) for a set angle of rotation. A schematic of this device is shown in Figure 12. Initially, the surface deforms elastically until part of the surface plastically deforms and the contact surfaces begin to slip against one another.

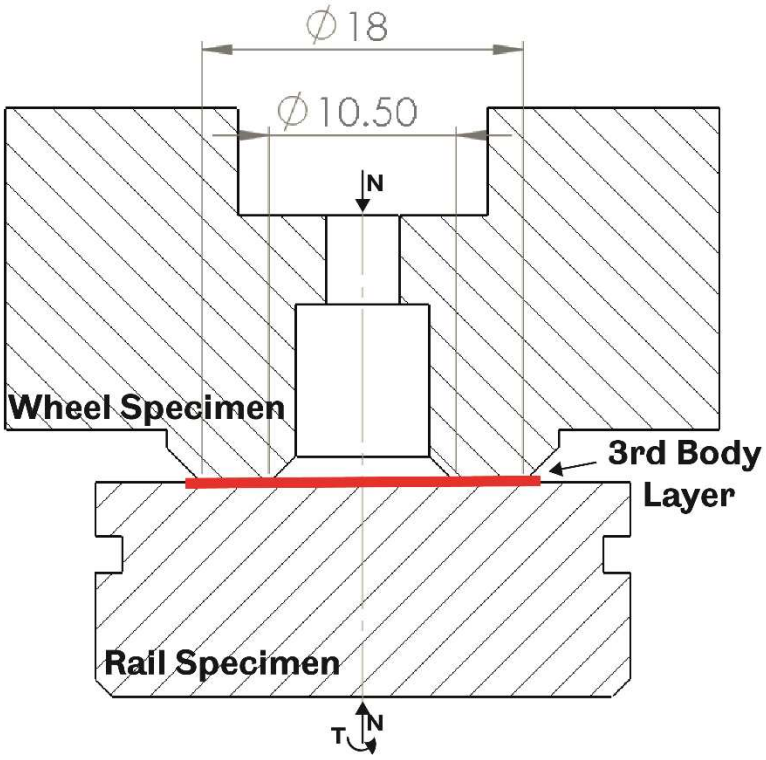


*Figure 12- Schematic of HPT Interface.*

Each set of tests used a ground surface to ensure repeatability, the rail specimens having an average $S_q$ measurement of 2.43 μm (standard deviation of 0.13 μm) and the wheel specimens having an average $S_q$ measurement of 2.57 μm (standard deviation of 0.20 μm). The specimens were run together to fully condition (shakedown) the surfaces and the third body material was then added to the contact. For the water and leaf extract, 100μL of liquid was added using a pipette. In sanded tests 0.025g of sand was hand placed, an example of this sand placement has been included in Figure 13; the mass of sand being used was consistent with the maximum density of sand allowable on UK railways [14], thereby meaning the HPT tests used a realistic amount of sand within the contact. The tested liquids include: distilled water and a leaf extract liquid which was produced by steeping leaves in water overnight and subsequently filtering out solid contaminants.

*Figure 13- Sand Placement on HPT Sample.*

Each sand type was tested in dry, wet, and leaf-extract contaminated conditions. The annular contact has an inner diameter of 10.5 mm and an outer diameter of 18 mm; a contact pressure of 900 MPa was used for all tests, with the maximum attainable torque being 1000 Nm. The

rotation angle used in each test was defined by the angle at which, for a point on the effective radius of friction (as defined in [31]), the sweep length was equal to 0.4 mm.

## 4.2 Dry Interface

In a dry interface all tested sands were shown to have little effect on the coefficient of traction; a plot of the coefficient of traction versus displacement has been included in Figure 14. The coefficient of traction for all runs reached values of 0.7-0.8. Two runs from both CE and DY sands did exhibit a slower rise in traction levels with displacement, though both runs eventually came to reside amongst traction values from other runs.

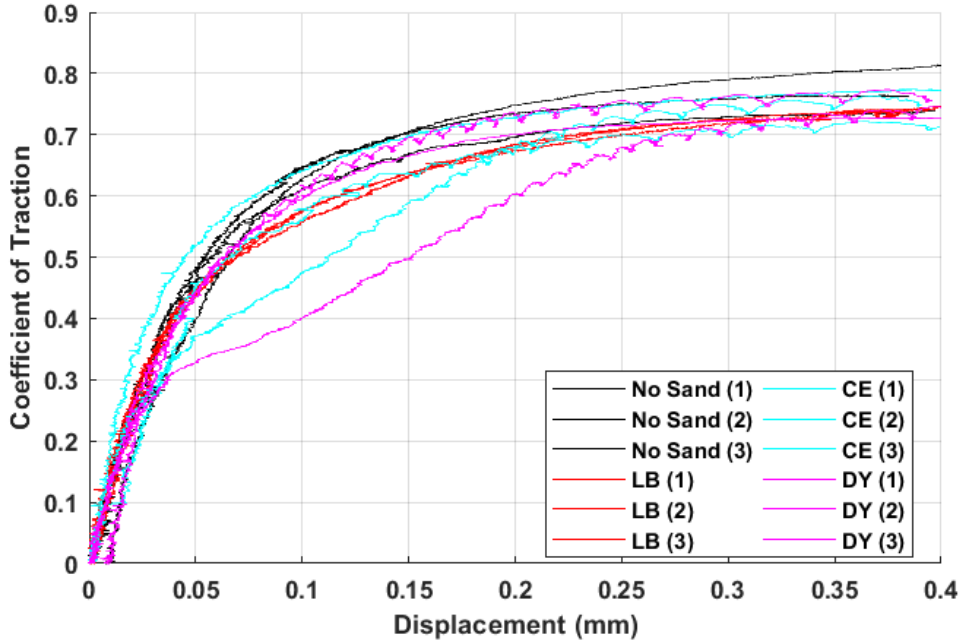


*Figure 14- Effect of Rail Sands on Traction in a Dry HPT Interface.*

## 4.3 Wet Interface

In the wet HPT interface the unsanded contact produced lower traction compared to dry tests as the water lubricated the contact; the peak coefficients of traction was ≤0.4. The decrease in traction after a maxima, occurred in all runs without sand. Both LB and CE rail sands increased traction in the contact whereas DY sand showed smaller improvements through two runs and no improvement for one run, as can be seen in Figure 15. In the case of CE and DY sands a peak traction was reached before decreasing to a steady value, similar to the peak seen in the unsanded low adhesion cases. LB sand acted differently in that it steadily increased till reaching a plateau at its peak traction.

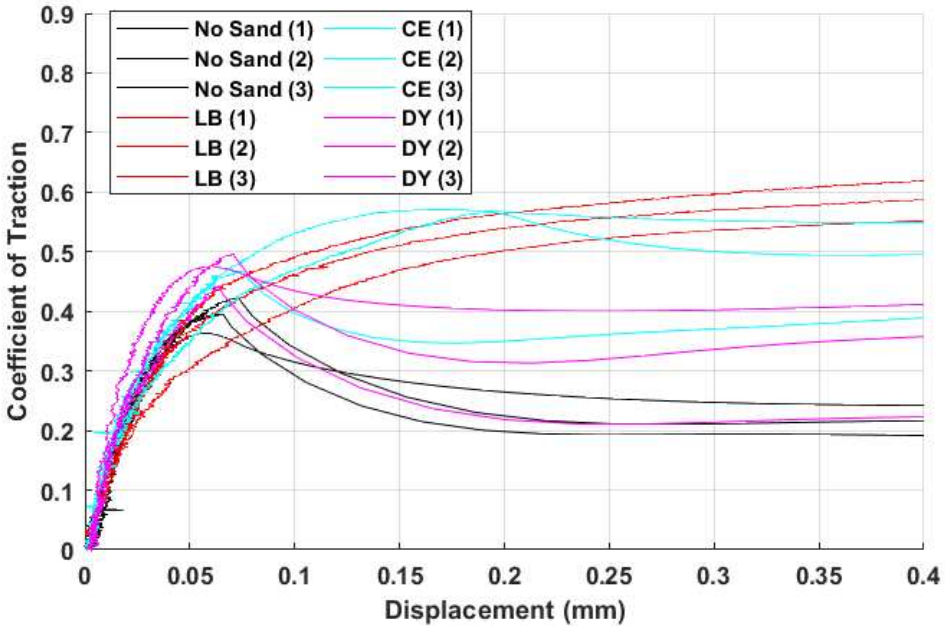


*Figure 15- Effect of Rail Sands on the Wet HPT Interface.*

## 4.4 Leaf Contaminated Interface

When leaf extract was applied to the contact the coefficient of traction slightly decreased compared to the wet contact, peak traction falling to 0.25-0.35; the ability of this leaf extract liquid lubricating the contact more than water alone was shown in work by Ishizaka et al. [6]. LB and CE sands increased the traction in the contaminated contact, with LB sand producing the larger peak coefficients of traction between 0.5-0.6 compared to 0.4-0.5 produced by CE sand, these results have been plotted in Figure 16. As before DY sand varied between showing little to no improvement in traction. The traction peaks produced by CE and DY sand in wet contacts also exist in the leaf extract contaminated contact indicating large slip events.

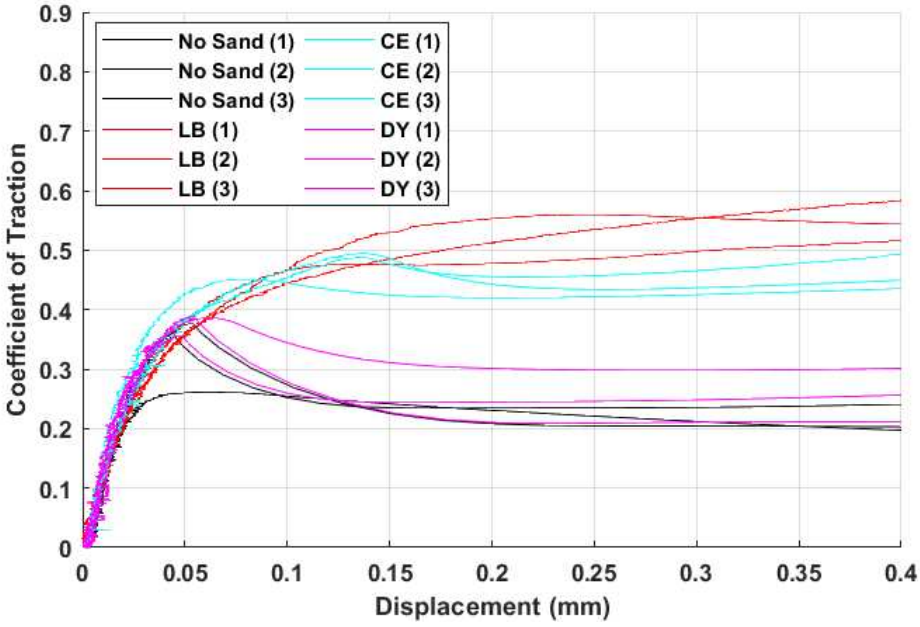


*Figure 16- Effect of Rail Sands on the Leaf Extract Contaminated HPT Interface.*

## 4.5 Roughness Data

Roughness measurements of the tested surfaces was analysed using the Alicona optical measurement device and analysed using built-in software. Two scans were taken for each tested wheel and rail specimen. Each 3D scan was taken over a 3.66x3.66 $mm^2$ area with a vertical resolution of 500 nm. The measure of roughness used in this paper was the RMS height, $S_q$, from a reference plane (calculated from a default function of the software).

Figure 17, Figure 18, and Figure 19 show the average roughness values of the wheel and rail specimens after testing in all contact conditions. In all cases, except for CE sand in wet, roughness was higher for the wheel specimen compared to the rail specimen, possibly due to the wheel material being softer [29].

From Figure 17 there was found to be little difference in $S_q$ between the unsanded and sanded contact in dry conditions, $S_q$ being about 10 µm in all cases.

Under wet conditions, roughness values (Figure 18), were increased with the presence of sand, however there was little difference found between the unsanded dry and wet cases. CE and DY sands gave larger roughness values than LB sand and all sands presented higher roughness values than seen in dry conditions.

When leaf extract was present in the contact (Figure 19) the unsanded contact was less rough than the sanded contact, similar to the wet contact. In the leaf contaminated case it appears that the larger sands produced higher values of roughness.

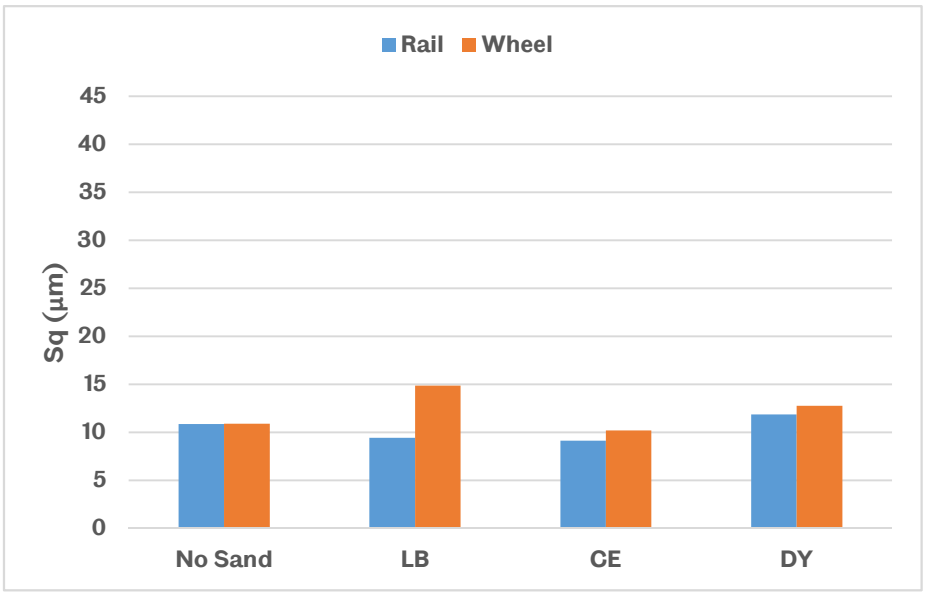


*Figure 17- Average Roughness Measurements from Dry Tests.*

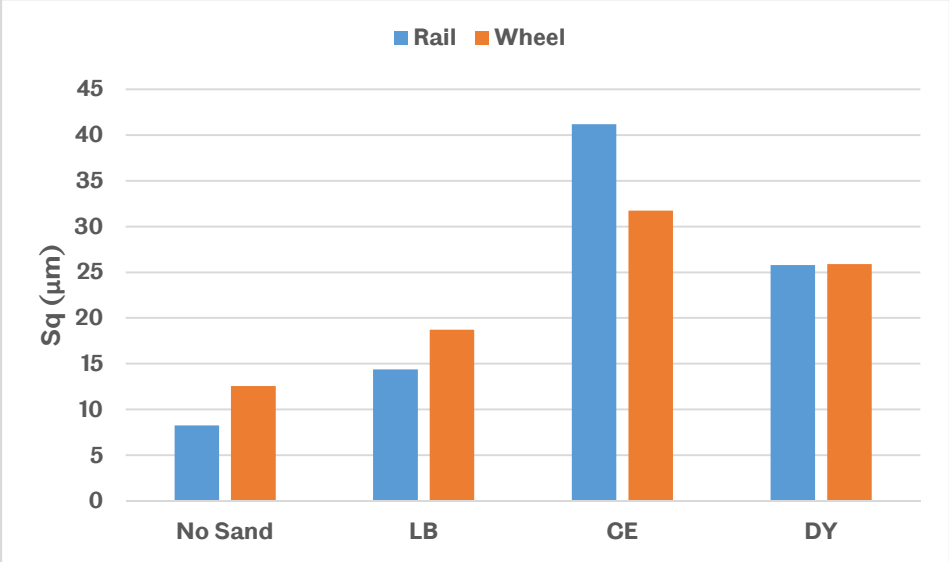


*Figure 18- Average Roughness Measurements from Wet Tests.*

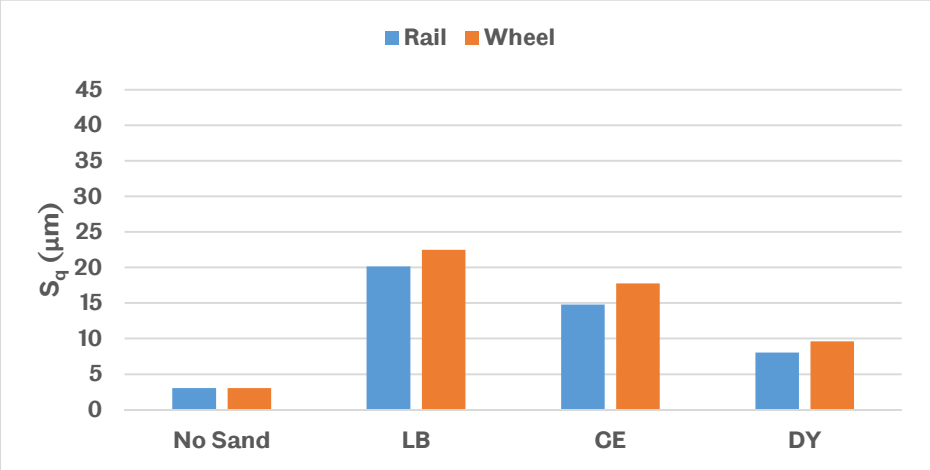


*Figure 19- Average Roughness Measurements from Tests with Leaf Extract.*

From the scans used to acquire roughness data an example image of a rail specimen surface was taken for each contact condition and included in Figure 20. Comparing the dry contacts, Figure 20 (a), (b), (c), (d), it can be seen the dry surfaces are very similar with the exception of (b) where a particle has indented and created a large crater, the only time this was observed on a dry surface. Comparing the unsanded cases, Figure 20 (a), (e), (i), the two low adhesion cases show much larger smoother areas than the dry case, with the wet conditions also showing signs of abrasion, possibly from wear debris. When LB and CE sand was introduced in the low adhesion cases, Figure 20 (f), (g), (j), (k), most conditions showed large areas with lower heights, suggesting particle indentation was occurring. When DY sand was applied to the contact, Figure 20 (h), (l), the amount of indentation occurring is either smaller or non-existent compared to the other sands.

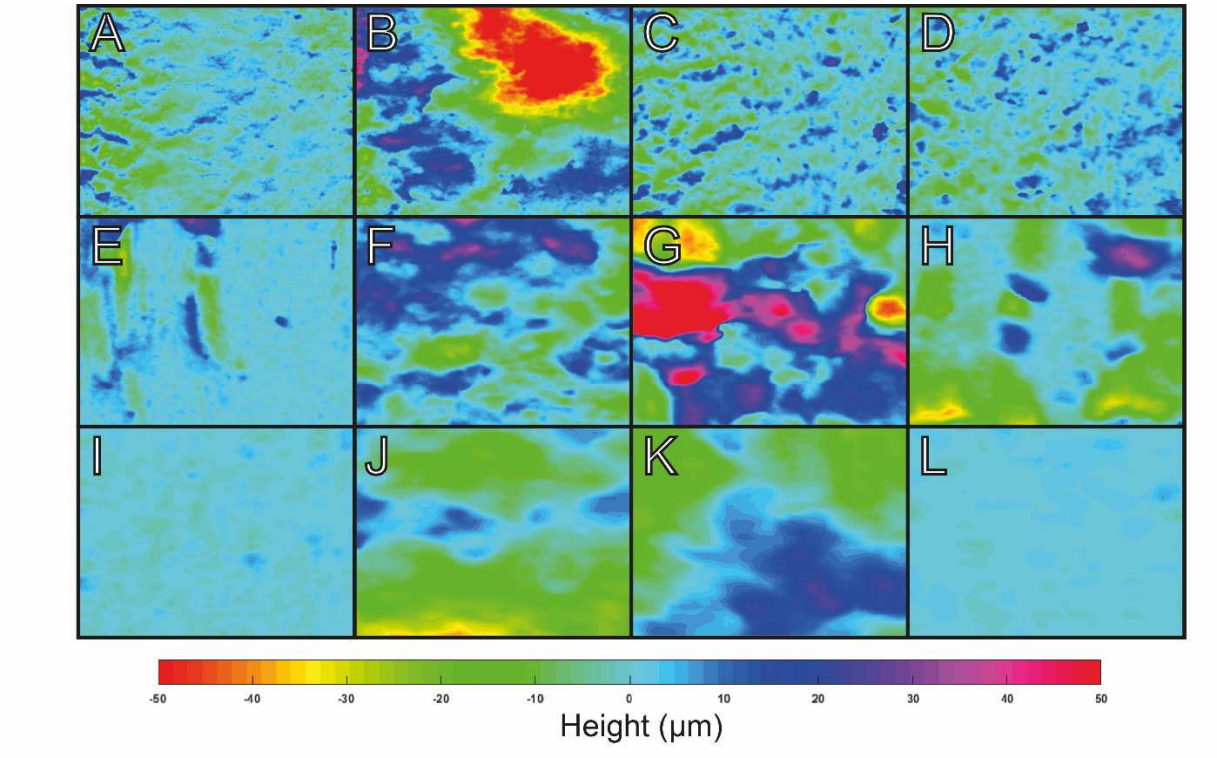


*Figure 20- Surfaces of Rail Specimens After Testing; (a) Dry Unsanded; (b) Dry LB; (c) Dry CE; (d) Dry DY; (e) Wet Unsanded; (f) Wet LB; (g) Wet CE; (h) Wet DY; (i) Leaf Unsanded; (j) Leaf LB; (k) Leaf CE; (l) Leaf DY.*

# 5 DISCUSSION

Results from the characterisation tests showed that particle size was the only prominent difference between the tested rail sands. This is not surprising as most rail sand is largely quartz based, both UK and German sand specifications call for quartz rich sand [14], [33], therefore little difference will exist between single particle characteristics. The differences amongst sands measured in the bulk characterisation tests can be attributed to the difference in particle morphology, illustrating how single particle characteristics can affect sander operation, as well as particle performance within the contact.

The characterisation framework presented in this paper can be improved by the addition of X-ray tomography to produce a 3D size and shape analysis of different particles, thus giving a more accurate picture of particle morphology and its effects on traction restoration. More particles will need to be tested to develop more links between particle properties and their effect on adhesion, in this case only inferences about the effect of particle size and, to a lesser degree, particle shape can be made.

In dry HPT tests very little difference was found between the sanded and unsanded contacts, possibly due to the lack of sand being retained in the contact upon crushing. The lack of difference in roughness in the dry case shows this as well as the similarity between Figure 20 (a), (c), (d). When sand was retained in the contact a large local indent was created, such as Figure 20 (b), it did not seem to have an effect on the rest of the contact.

The differences in particle morphology may help to explain the differences in traction coefficients in the HPT tests. The larger LB sand produced the largest traction coefficient in low adhesion conditions whereas the smaller DY sand produced little to no change. This trend was especially pronounced for the leaf contaminated contact compared to the wet contact.

Following the traction test, inspection of the surfaces shows that the wet contact has higher roughness values when unsanded in comparison to the leaf contact, possibly due to third body abrasion from wear debris. Possible explanations for this include:

- The leaf contaminated surfaces being protected by a small black leaf layer, characteristic to leaves on the line [6], therefore undergoing less surface damage and not producing as much wear debris as in the wet contact. Upon the application of sand into the wet contact, the wear debris in the system may change the effect of the applied sand particles, making the effect of sand in the contact more obvious for the leaf contaminated contact.
- The difference in wettability between the water and leaf extract liquid. It was observed during testing that the leaf extract liquid had greater wettability than distilled water, allowing sand particles to spread over the surface more effectively therefore ensuring the sand was active in more of the contact. Figure 20 supports this as the sanded leaf contaminated contacts had greater height consistency over the area.

The leaf contaminated contact showed that the larger sands created more roughness. This may be a result of the sands creating larger indents in the surface as they are crushed. The effect of these indents on the thin black leaf layer would be to break through the leaf layer causing more wheel-to-rail or wheel-to-sand-to-rail contacts.

# 6 CONCLUSIONS

Three sands commonly used in the rail industry (LB, CE, DY) were assessed in this paper for their effect on improving adhesion. The only discernible difference between the sands was in their size. Morphology characterisation found that: LB sand was the largest sand whereas DY sand was the smallest sand.

The HPT tests showed that all sands had little impact in dry conditions. LB and CE sands improved traction in low adhesion conditions, whereas DY sand had little to no impact. Roughness measurements of HPT samples post-testing showed that: in dry conditions sand had no impact on roughness due to the particles being expelled upon crushing, whereas in low adhesion conditions, the presence of sand increased roughness values. In addition, images of the unsanded wet surface showed evidence of 3$^{rd}$ body abrasion from wear debris, something which was absent in the leaf contaminated contact. The leaf contaminated contact showed a link between decreasing particle size and decreasing surface roughness. Two possible explanations were offered for the difference in behaviour between the sanded wet and leaf contaminated contacts: the presence of a protective leaf layer, and the greater wettability of the leaf extract liquid.

Future work will include:

- Improving morphology characterisation by using X-ray tomography to obtain 3D measurements of the particles.
- Expanding the types of particles being tested to determine more relationships between particle properties and tribological performance.
- An investigation into the mechanisms behind particle breakage within the contact.
- Assessing alternative ways of using leaves in the HPT contact to produce very low adhesion (<0.2) conditions.
- Using distinct element method techniques to model the HPT test.

## ACKNOWLEDGMENT

The authors would like to thank the UK Rail Safety and Standards Board (RSSB) for part funding and guiding the work in this paper. In addition, the authors would like to thank the Engineering and Physical Sciences Research Council (EPSRC) for also part funding this research. The second author is supported by the EPSRC (grant number EP/001766/1) as a part of 'Friction: The Tribology Enigma' Programme Grant (www.friction.org.uk), a collaboration between the Universities of Leeds and Sheffield. Lastly, the authors would like to thank Professor Ghadiri for his guidance whilst writing this paper.

## REFERENCES

[1] P. Gray, "T1107 Sander Trials Dissemination Event," 2018. [Online]. Available: https://www.rssb.co.uk/Pages/adhesion.aspx.

[2] C. R. Fulford, "Review of low adhesion research (T354) (RSSB Report)," 2004. [Online]. Available: https://www.sparkrail.org/Lists/Records/DispForm.aspx?ID=9539.

[3] Rail Accident Investigation Branch, "Autumn Adhesion Investigation Part 3: Review of adhesion-related incidents Autumn 2005 (RAIB Report)," 2007.

[4] T. M. Beagley and C. Pritchard, "Wheel/rail adhesion - the overriding influence of water," *Wear*, vol. 35, no. 2, pp. 299–313, 1975.

[5] L. Buckley-Johnstone, R. Lewis, K. Six, and G. Trummer, "Modelling and quantifying the influence of water on wheel / rail adhesion levels (RSSB Rport)," 2016. [Online]. Available: https://www.sparkrail.org/Lists/Records/DispForm.aspx?ID=24280.

[6] K. Ishizaka, S. R. Lewis, and R. Lewis, "The low adhesion problem due to leaf contamination in the wheel/rail contact: Bonding and low adhesion mechanisms," *Wear*, vol. 378–379, pp. 183–197, 2017.

[7] W. A. Skipper, A. Chalisey, and R. Lewis, "A Review of Railway Sanding System Research: Adhesion Restoration and Leaf Layer Removal," *Tribol. - Mater. Surfaces Interfaces*, vol. 12, no. 4, pp. 237–251, 2018.

[8] O. Arias-Cuevas, Z. Li, R. Lewis, and E. a Gallardo-Hernández, "Laboratory investigation of some sanding parameters to improve the adhesion in leaf-contaminated wheel–rail contacts," *J. Rail Rapid Transit*, vol. 224, no. 3, pp. 139–157, 2010.

[9] O. Arias-Cuevas and Z. Li, "Field investigations into the adhesion recovery in leaf-contaminated wheel–rail contacts with locomotive sanders," *J. Rail Rapid Transit*, vol. 225, no. 5, pp. 443–456, 2011.

[10] O. Arias-Cuevas, Z. Li, and R. Lewis, "A laboratory investigation on the influence of the particle size and slip during sanding on the adhesion and wear in the wheel-rail contact," *Wear*, vol. 271, no. 1–2, pp. 14–24, 2010.

[11] W. Wang, T. Liu, H. Wang, Q. Liu, M. Zhu, and X. Jin, "Influence of friction modifiers on improving adhesion and surface damage of wheel/rail under low adhesion conditions,"

*Tribiology Int.*, vol. 75, pp. 16–23, 2014.

[12] P. R. Cooper, “An investigation into the relationship between the Particle Size and the Frictional Performance of Sand (IM-ADH-011) (British Rail Report),” 1972. [Online]. Available: https://www.sparkrail.org/Lists/Records/DispForm.aspx?ID=10483.

[13] F. G. R. Zobel, “Development of Remedies for Poor Adhesion (IM-ADH-019) (British Rail Research),” 1974. [Online]. Available: https://www.sparkrail.org/Lists/Records/DispForm.aspx?ID=9038.

[14] Rail Safety and Standards Board, “GMRT2461 Sanding Equipment (Issue 2),” 2016. [Online]. Available: https://www.rssb.co.uk/rgs/standards/GMRT2461 Iss 2.pdf.

[15] ASTM, “ASTM C702-18: Standard Practice for Reducing Samples of Aggregate to Testing Size.” 2018.

[16] T. Allen, *Particle Size Measurement, 3rd Edition*. Chapman & Hall, 1981.

[17] S. Haeri, Y. Wang, O. Ghita, and J. Sun, “Discrete element simulation and experimental study of powder spreading process in additive manufacturing,” *Powder Technol.*, 2017.

[18] W. Nan *et al.*, “Jamming during particle spreading in additive manufacturing,” *Powder Technol.*, 2018.

[19] S. Nadimi and J. Fonseca, “A micro finite-element model for soil behaviour: numerical validation,” *Géotechnique*, no. June, pp. 1–6, 2017.

[20] W. C. Oliver and G. M. Pharr, “An improved technique for determining hardness and elastic modulus using load and displacement sensing indentation experiments,” *J. Mater. Res.*, vol. 7, no. 6, pp. 1564–1583, 1992.

[21] N. P. Daphalapurkar, F. Wang, B. Fu, H. Lu, and R. Komanduri, “Determination of Mechanical Properties of Sand Grains by Nanoindentation,” *Exp. Mech.*, vol. 51, no. 5, pp. 719–728, 2011.

[22] S. R. Lewis, S. Riley, D. I. Fletcher, and R. Lewis, “Optimisation of a Railway Sanding System for Optimal Grain Entrainment into the Wheel/Rail Contact,” *J. Rail Rapid Transit*, vol. 232, no. 1, pp. 43–62, 2016.

[23] U. Zafar, C. Hare, A. Hassanpour, and M. Ghadiri, “Drop test: A new method to measure the particle adhesion force,” *Powder Technol.*, vol. 264, pp. 236–241, 2014.

[24] K. L. Johnson, K. Kendall, and A. D. Roberts, “Surface Energy and the Contact of Elastic Solids,” *Proc. R. Soc. A Math. Phys. Eng. Sci.*, 1971.

[25] R. Lewis and J. Masing, “Static wheel / rail contact isolation due to track contamination,” *J. Rail Rapid Transit*, vol. 220, no. 1, pp. 43–53, 2006.

[26] H. M. B. Al-Hashemi and O. S. B. Al-Amoudi, “A review on the angle of repose of granular materials,” *Powder Technol.*, vol. 330, pp. 397–417, 2018.

[27] D. Geldart, E. C. Abdullah, A. Hassanpour, L. C. Nwoke, and I. Wouters, “Charcterization of Powder Flowability Using Measurement of Angle of Repose,” *China*

*Particuology*, vol. 4, no. 3–4, pp. 104–107, 2006.

[28] A. Hassanpour and M. Ghadiri, “Distinct element analysis and experimental evaluation of the Heckel analysis of bulk powder compression,” *Powder Technol.*, vol. 141, no. 3, pp. 251–261, 2004.

[29] R. Lewis and R. S. Dwyer-Joyce, “Wear at the wheel/rail interface when sanding is used to increase adhesion,” *J. Rail Rapid Transit*, vol. 220, no. 1, pp. 29–41, 2006.

[30] L. E. Buckley-Johnstone *et al.*, “Assessing the impact of small amounts of water and iron oxides on adhesion in the wheel/rail interface using High Pressure Torsion testing,” *Tribol. Int.*, vol. 135, pp. 55–64, 2018.

[31] M. D. Evans, “Performance Assessment of Friction Management products in the Wheel-Rail Interface,” 2017.

[32] A. Meierhofer, “A New Wheel-Rail Creep Force Model based on Elasto-Plastic Third Body Layers,” 2015.

[33] DB/EBA/VDB/VDV Working Group, “Supplementary Regulation No. B 011 to ‘Sanding,’” 2016.